# Optical Properties and Photo-Oxidation of Tetraphenylethene-Based Fluorophores

**ARTICLE** *in* CHEMISTRY - A EUROPEAN JOURNAL · DECEMBER 2012

Impact Factor: 5.73 · DOI: 10.1002/chem.201202715 · Source: PubMed



**3 AUTHORS:**

Matthew P Aldred
Huazhong University of Science and Techn…
**49** PUBLICATIONS **919** CITATIONS
SEE PROFILE

Chong Li
Huazhong University of Science and Techn…
**19** PUBLICATIONS **293** CITATIONS
SEE PROFILE

Ming-Qiang Zhu
Huazhong University of Science and Techn…
**69** PUBLICATIONS **1,601** CITATIONS
SEE PROFILE

CHEMISTRY
A EUROPEAN JOURNAL

FULL PAPER

DOI: 10.1002/chem.201202715

# Optical Properties and Photo-Oxidation of Tetraphenylethene-Based Fluorophores

**Matthew P. Aldred, Chong Li, and Ming-Qiang Zhu*[a]**

**Abstract:** We report the optical properties of tetraphenylethene (TPE) and other TPE derivatives functionalised with an octyl group (TPE-OCT) and polyethyleneglycol group (TPE-PEG) in the side chain. We compared TPE-OCT and TPE-PEG with TPE in both organic solvents and under aqueous conditions. All materials exhibit aggregation-induced emission, however, uncommonly, TPE-PEG seems to aggregate in aqueous solution with enhanced photoluminescence quantum efficiency (PLQE) relative to that in organic solvents. All three materials can be photo-oxidised in solution to their diphenylphenanthrene derivative by irradiation with UV light (at both $\approx 1$ and $\approx 5\ mW\,cm^{-2}$), with a subsequent enhancement in PL efficiency. The electron-donating ether group increases the rate of oxidation relative to bare TPE and also photo-oxidation was shown to be solvent and concentration dependent. Finally, photo-oxidation was also demonstrated in the aggregate state.

**Keywords:** aggregation · biosensors · luminescence · optical physics · oxidation

## Introduction

Mainly as a result of the pioneering research by Tang's group, in recent years tetraphenylethene (TPE) has become the focus of much attention, primarily due to its aggregation-induced emission (AIE) properties.[1] Although there have been a number of aryl–ethene-based molecules reported to exhibit AIE properties,[2] TPE-based materials have received the most attention[3] owing to their well-defined AIE properties, high solid-state fluorescence quantum yields and ease of synthesis. TPE and TPE-based materials are highly emissive in the "aggregate" state compared with their weak emission in solution. The aggregate state has been shown to form in the solid state (thin film or powder), nanoparticle state and in aqueous solutions upon binding with "guests" such as biomolecules or ions. Therefore, the AIE phenomenon can be investigated by comparing the fluorescence changes in solution and the aggregate state. The reprecipitation method using a solvent and anti-solvent, in which nanoparticles are formed at low fluorophore concentration and high water content, has been widely used in the literature. Here, the addition of an anti-solvent (most commonly water) at a critical concentration causes nano-precipitation that enhances the photoluminescence intensity sharply owing to restriction of internal motions. In addition, a comparison of the solution and nanoparticle/solid-state photoluminescence quantum efficiencies (PLQE) can be used. Although the term "aggregation" implies that the mechanism for emission enhancement is intermolecular, in fact the AIE of TPE and TPE-based molecules is due to intramolecular effects.[4] It is no surprise that, owing to their high PLQE in the solid state, TPE-based materials have found great promise in organic light-emitting diodes (OLEDs)[5] like the analogous phenylenevinylene-based fluorophores.[6] Also, another area in which TPE has found increased attention over recent years and has been intensively researched is sensors, that is, bio-/chemosensors[7] and ion sensors.[8] The experiments performed in biosensing research are typically in aqueous solutions, in which the TPE molecule has been derivatised to enable dissolution in water. The environmental surroundings of TPE are crucial in determining its fluorescence behaviour.

The photophysics of TPE have been investigated previously,[9] however, despite its newly discovered AIE properties and recent rise in popularity, the susceptibility of TPE-based materials to photo-oxidation has received little attention.[10] TPE and *cis*-stilbene are similar in terms of structure and photochemistry, however, the photochromism[11] and photo-oxidation[12] of stilbene and stilbene-based materials have been widely researched. Stilbene undergoes *trans–cis* isomerisation following irradiation with UV light, in which subsequent photocyclisation of *cis*-stilbene forms *trans*-4*a*,4*b*-dihydrophenanthrene that is unstable and, if not trapped, reverts back to *cis*-stilbene. However, if trapped by means of oxidation, dihydrophenanthrene can be oxidised to yield phenanthrene, which is irreversible and detrimental to the photochromism of *cis*-stilbene (Scheme 1). Owing to the intense research of TPE in recent years and a subsequent plethora of published papers, we thought it worthy to further investigate its photostability. Therefore, herein we

[a] Dr. M. P. Aldred, C. Li, Prof. M.-Q. Zhu
Wuhan National Laboratory of Optoelectronics (WNLO)
Huazhong University of Science and Technology (HUST)
Wuhan, Hubei 430074 (P.R. China)
Fax: (+86) 27-87793419
E-mail: mqzhu@hust.edu.cn

Supporting information for this article is available on the WWW under http://dx.doi.org/10.1002/chem.201202715.

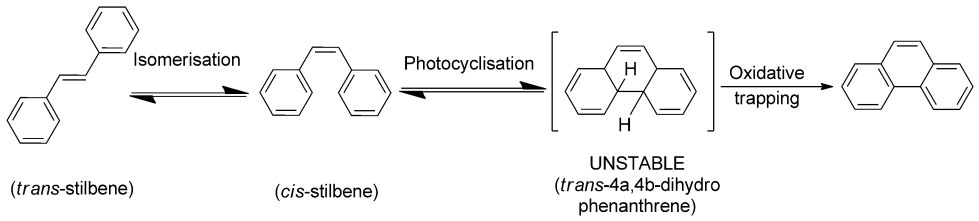


Scheme 1. Photocyclisation and oxidation of bis-stilbene.

report some optical properties and photo-oxidation experiments of TPE. We have found that TPE and analogous ether-functionalised TPE compounds are dramatically photo-oxidised in organic solvents, aqueous solutions and in the nanoparticle state. This photo-oxidation should provide an incentive for improving the photostability of TPE-based materials, especially in the areas of sensory research, and encourage the design and synthesis of novel TPE structures with improved photostability.

## Results and Discussion

**Steady-state absorption and emission**: The TPE derivatives were synthesised using standard synthetic procedures, according to Scheme 2.

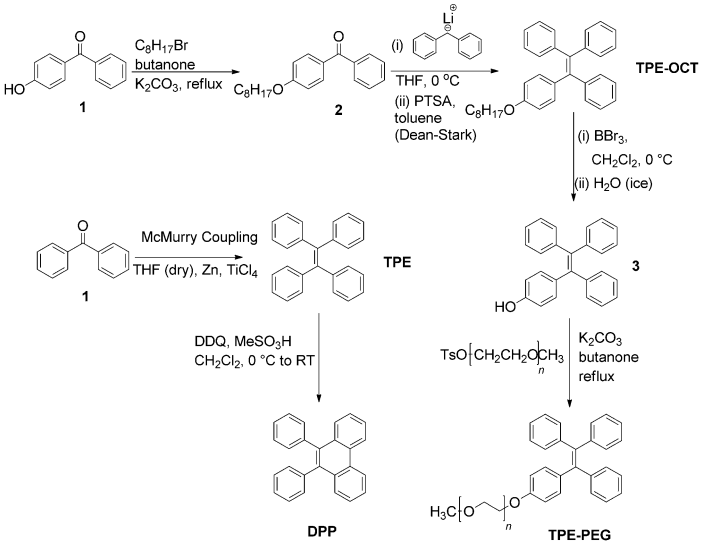


Scheme 2. Synthetic routes to TPE and its derivatives TPE-OCT, TPE-PEG and DPP.

The emission from solutions of the TPE materials in THF was not detectable owing to considerable quenching. From the PLQE data shown in Table 1, it is clear that all the TPE derivatives—including TPE functionalised with an octyl group (TPE-OCT) or a polyethyleneglycol group (TPE-PEG) in the side chain—exhibit AIE behaviour. This can be further confirmed by solvent (THF)–anti solvent (water) experiments, in which a low concentration of fluorophore in THF ($10^{-5}$ M) is added to water with a final water/THF (v/v) ratio of 99:1. After vigorous agitation of the solution, the nanoparticle solution appears transparent and homogeneous with no sign of precipitation. Owing to nanoprecipitation, the molecules aggregate enough to restrict internal motions and consequently the PL intensity (Figure 1) and PLQY values are enhanced. TPE exhibits the highest fluorescence efficiency (13%) of the fluorophores. The low PLQE values for TPE-OCT (1.7%) and TPE-PEG (1.5%) reflect the detrimental effect of the long alkyl side chains, which probably decrease the aggregation between the aromatic cores and consequently the internal motions are not restricted efficiently. 9,10-Diphenylphenanthrene (DPP) shows classical aggregation-caused quenching (ACQ) behaviour and the PLQE values in THF (5.3%) are higher than those in the nanoparticle state (1.2%). However, the absolute PLQE values are expected to be much higher, owing to the over estimation of the UV absorbance caused by the light scattering of the nanoparticles.[13] The AIE phenomenon that exists in TPE-based materials is due to the reduction of torsional and rotational motions and out-of-plane bending vibrations; these internal motions around the ethylenic bond and the bonds connecting the phenyl rings to the ethylenic double bond have both been shown to contribute significantly.[8c,f] In fact, the effect of internal motions on the fluorescence properties of TPE-based materials, such as TPE and stilbene, has been known for a long time.[8] However, taking

Table 1. Optical properties of TPE, DPP, TPE-OCT and TPE-PEG.

| | $\lambda_{abs}$ [nm] | $\lambda_{em}$ [nm] | | | $\Phi_F$ [%] | |
|---|---|---|---|---|---|---|
| | | solution | aggregate | solid | solution[a] | aggregate[b] |
| TPE | 238, 308 | n.d.[c] | 468 | 448 | 0.5 | 13 |
| DPP | 258, 301, 351 | 355, 373, 392 | 474 | 474 | 5.3[b] | 1.2 |
| TPE-OCT | 317 | n.d.[c] | 484 | 474 | 0.4 | 1.7 |
| TPE-PEG | 316 | n.d.[c] | 485 | 492 | 0.3 | 1.5 |

[a] $\Phi_F$ estimated by the optical dilution method. The standard is anthracene (0.27 in ethanol) unless stated otherwise. [b] The standard is quinine sulfate (0.54 in 0.1 M $H_2SO_4$). PL in solution using THF as the solvent ($\lambda_{ex}$ = 310); TPE and DPP in the solid state ($\lambda_{ex}$ = 310); TPE-OCT and TPE-PEG in the solid state ($\lambda_{ex}$ = 330); aggregate is measured in a 99% water/THF solvent mixture. The solid-state emission was recorded from the powder or oil (TPE-PEG). [c] n.d. = not determined.

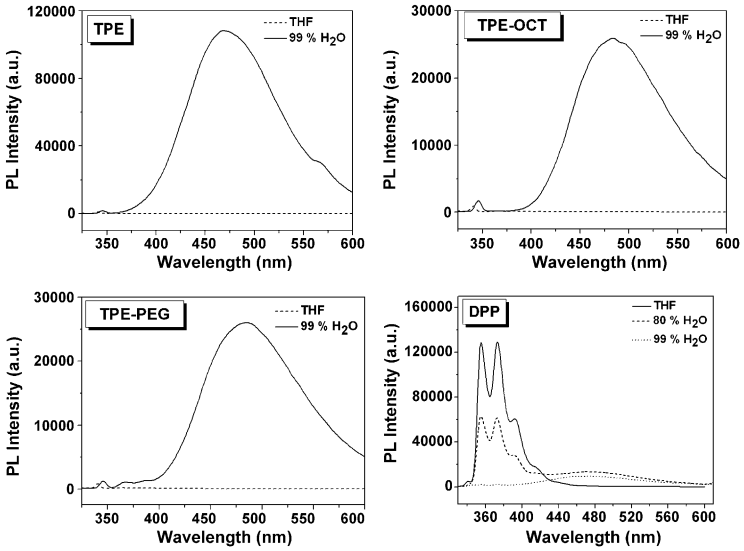


Figure 1. THF/water solvent mixture experiments to investigate the emission properties of the fluorophores in the "isolated" and "aggregated" states. Excitation = 310 nm, concentration = $10^{-5}$ M.

advantage of the extremes in fluorescence properties, that is, quenching in the "monomeric" state and emission enhancement in the aggregate state, within applied science for useful applications, has only recently been demonstrated.[14] Although TPE-OCT and TPE-PEG differ by their insoluble and soluble nature in water, respectively, interestingly their emission profiles in 99% water–THF are similar, which indicates a degree of "aggregation" of TPE-PEG in water owing to phase segregation of the hydrophilic PEG side chains and the hydrophobic TPE core. TPE-PEG in aqueous solution also exhibits a long-wavelength emission peak that is similar to its solid state and to TPE and TPE-OCT in the nanoparticle state. The $PL_{max}$ in the solid state is very similar to that in the nanoparticle.

From previous studies we know that the TPE group in solution exhibits unrestricted internal bond motions resulting in poor fluorescence efficiencies. When TPE is connected to other aromatic cores it generally has a strong effect and consequently most reported TPE-based materials, even with complex structural architectures, still exhibit low fluorescence quantum efficiencies in solution.[4,15] This is in sharp contrast to the "aggregate" or solid state, where the fluorescence efficiencies are dramatically enhanced due to restriction of intramolecular rotation (RIR). Therefore, TPE-based materials in the "aggregate" and solid state are usually efficient light emitters. The optical properties of TPE-based materials show large Stokes shifts in the solid state compared with small Stokes shifts in the solution state. This has previously been explained by the extremes in the structural conformations of the TPE molecule in solution and in the solid state.[4] Accordingly, there is a big difference in the solution and solid-state emission peak wavelengths. The TPE-based fluorophores reported here also follow these same characteristics. Most of the published TPE-based materials and the fluorophores here exhibit broad emission spectra that are considerably redshifted in the solid state. From these characteristics at first glance one would suspect excimer formation, however, the fluorescence efficiency is higher than that in the solution state, which is opposite to excimer formation, and in most cases drastically quenches the fluorescence. Also, compared to the solid state there is negligible change in the emission band structure and wavelength after dispersing TPE in polymethylmethacrylate (PMMA) at low to medium concentrations (Figure 2), which

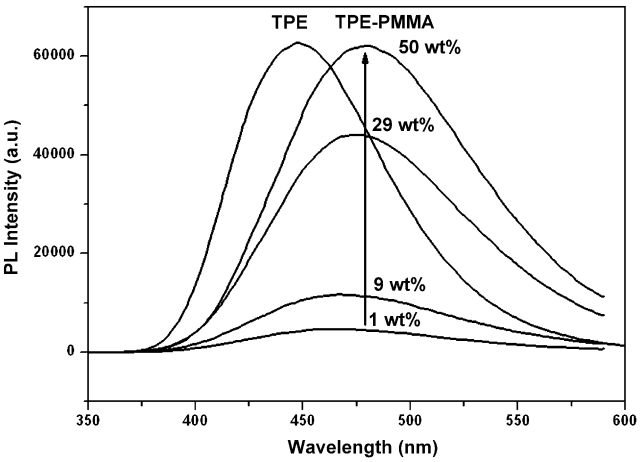


Figure 2. PL spectra of pure TPE and TPE-PMMA at different wt% concentrations of TPE.

suggests that intermolecular affects are not governing the emission properties to a considerable extent. The blueshift in emission wavelength of TPE in the solid state relative to TPE dispersed in a PMMA matrix is probably due to the morphology, in which TPE in the solid state is crystalline but has an amorphous morphology when dispersed in PMMA. In this respect, TPE in the amorphous state exhibits a more planar conformation than the more twisted conformation in the crystalline state. This blueshift has been reported by other research groups.[5d] To further confirm this difference in emission of the amorphous and crystalline states we prepared thin films of 80 wt% TPE in PMMA on a quartz substrate and compared the emission spectra before and after thermal treatment (Figure 3).

Before thermal treatment the film can be regarded as amorphous owing to its high transparency and glassy texture, which is facilitated by the small amount of PMMA. After thermal treatment of this same film by heating just below the glass transition temperature ($T_g$) of PMMA, at approximately 100 °C, the resulting film crystallises and exhibits an opaque texture. The emission of the resulting amorphous state is 480 nm and is redshifted by 32 nm relative to the crystalline state (448 nm). In contrast, the PL emission of DPP remains unchanged in the solid state relative to when it is dispersed in a PMMA matrix, which suggests that there is negligible change in structural conformations of DPP in both the amorphous and crystalline states.

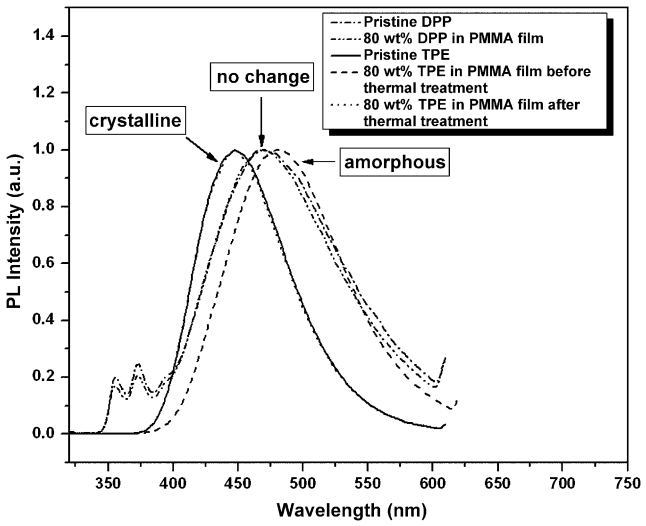


Figure 3. PL spectra of TPE in the pure form and in a PMMA matrix (80 wt%) before and after thermal treatment. Also DPP in pure form and in a PMMA matrix (80 wt%).

An interesting comparison is the emission properties of DPP. Here, two of the phenyl rings are "locked", which reduces the internal bond motions and as a result should increase the PLQE in solution. Indeed, the PLQE is enhanced more than tenfold from 0.5 (TPE) to 5.3% (DPP) and upon addition of water the PL intensity is reduced due to ACQ. A comparison of the "monomeric" and "aggregate" PL spectra of TPE and DPP (Figure 1) clearly illustrates both AIE and ACQ phenomena in analogous materials differing by reducing its internal motions. The low-energy emission band at 474 nm was further investigated to understand its origin. Figure 4 shows a comparison of the PL spectra of DPP in solution (THF), solid state and in a PMMA matrix at 9 wt%. In contrast to TPE, it is clear that the low-energy emission band of DPP in the solid state is largely due to intermolecular effects. Excimers in DPP-type materials have been demonstrated before.[16]

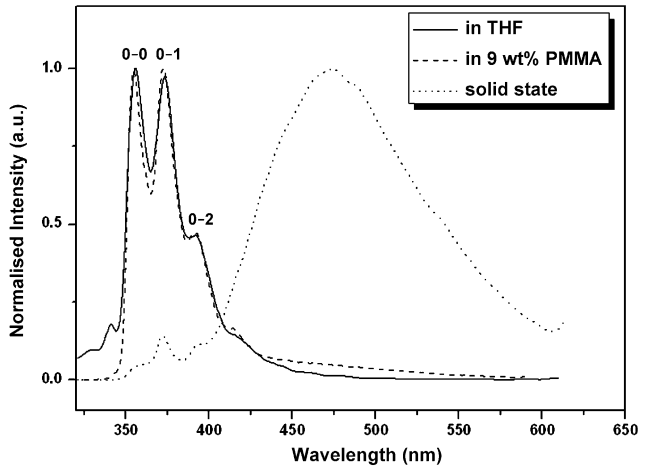


Figure 4. A comparison of the PL spectra of DPP in solution (THF), a PMMA matrix at 9 wt% and the solid state.

**Photo-oxidation behaviour (solution and nanoparticle state)**: During PL investigations of TPE we accidently observed that well-defined vibronic peaks in the range 350–400 nm increased upon repeated measurement. These peaks are reminiscent of phenanthrene and led us to the conclusion that photocylisation and photo-oxidation were taking place under our experimental conditions. This sensitivity to UV light encouraged us to further investigate the photo-oxidation of TPE-based fluorophores upon UV-light exposure. Oxidation of stilbene-type molecules is well known and has been used extensively with respect to photochemistry and as a synthetic tool. The latter was made possible by using iodine as the catalyst, in which large-scale oxidations can be carried out, and is most commonly known as the Mallory reaction ($h\nu$ and $I_2$)[17] or the Katz-modified Mallory reaction (using methyloxirane as the scavenger).[18]

By using our fluorescence spectrofluorometer, photo-oxidation kinetic measurements of TPE, TPE-OCT and TPE-PEG in different solvents were performed (Figure 5A), whereby the emission at a chosen wavelength was followed over a period of time at fixed excitation and emission wavelengths. Typically, the excitation wavelength was the maximum absorption wavelength ($\lambda_{abs}$), the emission wavelength was the maximum emission wavelength ($\lambda_{em}$) and the experiments were performed under ambient conditions using dry/purified solvents. Although the photo-oxidation tendency can be curbed by using lower-energy excitation wavelengths (i.e., away from its maximum absorbance), this is of course at the expense of its maximum potential brightness, therefore, the excitation wavelength at $\lambda_{abs}$ was used. The power of the light source was approximately 1 mW cm$^{-2}$. After 2 h of irradiation the emission spectra of TPE and TPE-OCT in hexane and THF exhibit defined emission bands, which is reminiscent of phenanthrene (Figure 5B–E). The emission spectrum of TPE in hexane is noticeably different from that in THF, with a broad emission peak at 540 nm, which is more redshifted than that in the solid state. Similar emission characteristics of oligo-fluorenes end-capped with TPE in hexane have also been demonstrated previously.[4] This unusual emission behaviour could be due to excimer formation in solution, however, this seems unlikely. Firstly, because the oligo-fluorene end-capped TPE compounds exhibit structural features that would essentially prevent excimers owing to the long alkyl chains at the fluorene 9-position. Secondly, TPE is non-planar, which should prevent the close intermolecular packing necessary for excimer formation. Significant spectral shifts in emission at different temperatures in 3-methylpentane have been attributed to different structural geometries of TPE.[9c] Therefore, the most likely explanation is due to different geometrical configurations of the TPE core in hexane, which seems to be a more planar configuration. The PL spectra of TPE-OCT and TPE-PEG in 99% water/THF (Figure 5F,G) are different because the molecules in the initial state are "ag-

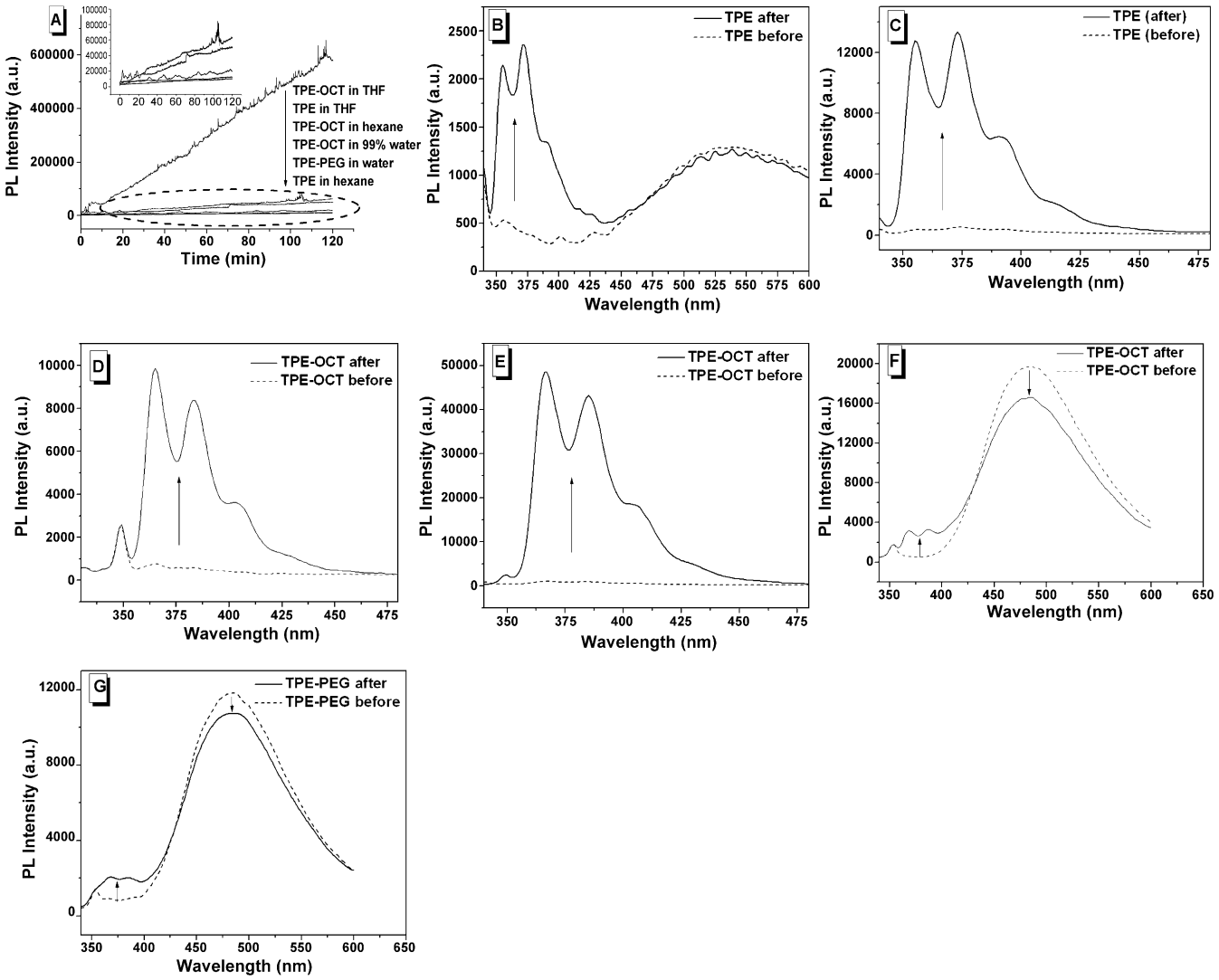


Figure 5. A) The kinetic scans of TPE, TPE-OCT and TPE-PEG in different solvents at a concentration of $10^{-5}$ M, during 2 h of UV-light irradiation. PL spectra of TPE in B) hexane, C) THF; of TPE-OCT in D) hexane, E) THF; of TPE-OCT in F) 99% water/THF; and of TPE-PEG in G) 99% water/THF under repeated UV-light exposure (UV max, $\approx$1 mW cm$^{-2}$). Concentration = $10^{-5}$ M.

gregated", compared to the "monomeric" emission in THF and hexane. Therefore, the broad emission peak around 470 nm at 0 s decreases as the irradiation time elapses owing to the depletion of TPE-OCT and TPE-PEG and perhaps the resulting lower PL efficiencies of the oxidised TPE-OCT and TPE-PEG aggregate. Unlike DPP, the oxidation forms of TPE-OCT/TPE-PEG seem to form fewer excimeric species than DPP in the aggregate state (see below). The slight increase of the defined emission peaks around 368 and 387 nm is probably due to the emission from the oxidation product (phenanthrene). The kinetic scans demonstrate three features about the rate of oxidation: 1) TPE-OCT > TPE, 2) THF > hexane and 3) solution > "aggregate"/aqueous solution. In all cases the photo-oxidation during the 2 h irradiation was incomplete owing to the low power ($\approx$1 mW cm$^{-2}$) of the light source. Due to the incomplete photo-oxidation, especially in the aggregate state, we further carried out some photo-oxidation tests (Figure 6) for TPE, TPE-OCT and TPE-PEG at 99% water/THF with higher power UV-light irradiation ($\approx$5 mW cm$^{-2}$).

During the photo-oxidation of TPE, the aggregate emission at 468 nm decreases and after 20 min is undetectable. This is due to the depletion of TPE and the subsequent lower fluorescence efficiency of DPP in the aggregate state, which is most likely an excimer. In comparison, the broad emission peak at 484 nm for TPE-OCT during photo-oxidation also rapidly decreases, but with a slight increase of the defined peaks at 368 and 387 nm. These defined peaks are most likely due to the phenanthrene core from TPE-OCT oxidation. The absence of these peaks during TPE oxidation (i.e., for DPP) suggests that excimer formation in oxidised TPE-OCT is much less than in TPE, because of the long octyl side chain that prevents sufficient aggregation that is needed for excimer formation. TPE-PEG behaves similar in that the broad emission peak around 485 nm also decreases upon UV-light irradiation, however, the emission peaks at

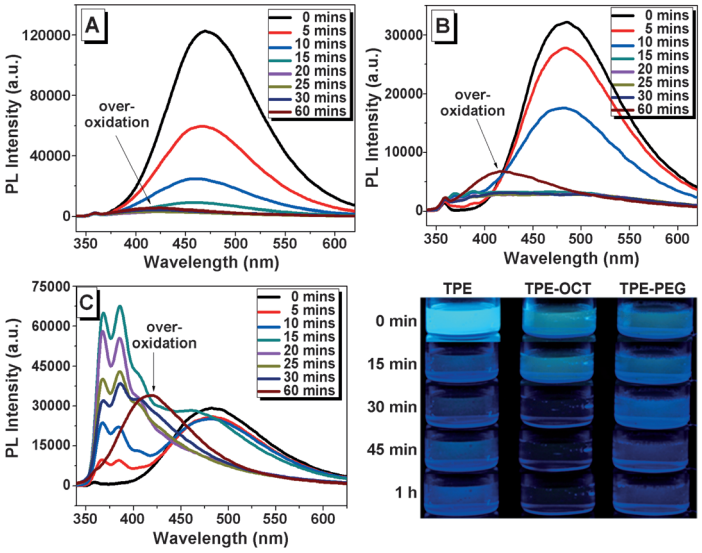


Figure 6. PL spectra of A) TPE, B) TPE-OCT and C) TPE-PEG in 99% water/THF ($10^{-5}$ M) with UV irradiation = 302 nm (≈5 mW cm$^{-2}$), excitation = 310 nm; and the corresponding photos excited over 302 illumination.

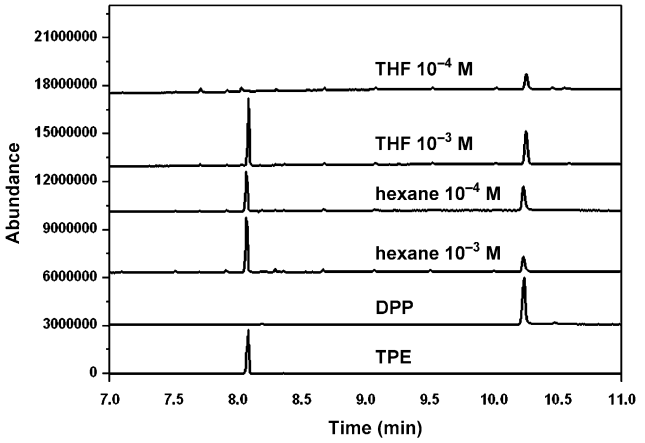


Figure 7. Gas chromatograms of TPE in THF and hexane after 4 h UV-light exposure at 302 nm (≈5 mW cm$^{-2}$). For reference, GC traces for pure TPE and DPP are also shown.

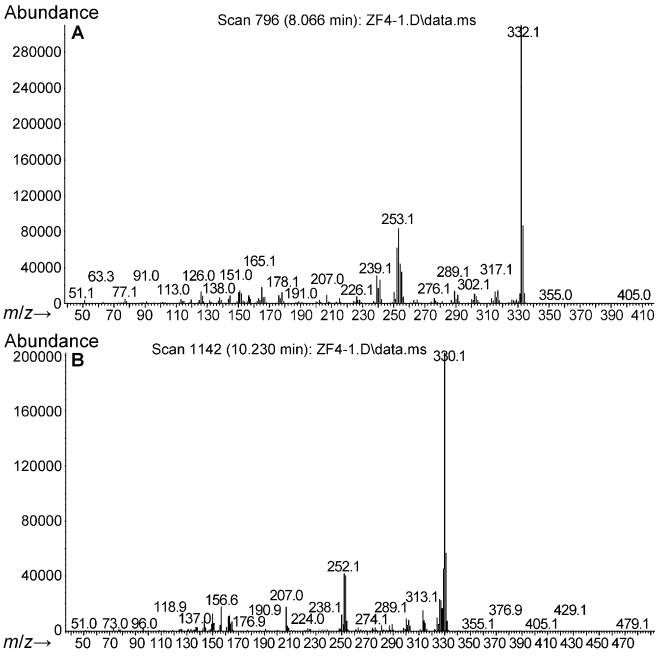


Figure 8. Typical ESI mass spectra from GC-MS analysis of A) TPE in hexane or THF after 4 h UV-light exposure ($[M]^+ = 332$) and B) DPP in hexane or THF after 4 h UV-light exposure ($[M]^+ = 330$).

368 and 386 nm show a large increase upon further light exposure. This suggests that its oxidised form exhibits higher fluorescence efficiency than the oxidised forms of TPE and TPE-OCT owing to the even longer PEG side chain, which prevents significant aggregation and perhaps because of its good solubility in aqueous media. One important feature of the TPE and TPE-OCT photo-oxidation is the transformation of materials that are AIE active into materials that exhibit ACQ. In all cases, over-oxidation occurs with a noticeable change in the emission spectra and the manifestation of an undefined peak at 424, 417 and 420 nm, for TPE, TPE-OCT and TPE-PEG, respectively. This over-oxidation does not occur for TPE in THF or hexane (see below), which suggests that it is accelerated in aqueous media. The low concentration of this species made it difficult to investigate its identity, however, it is most likely diphenyldibenzofulvene and/or dibenzo[*g*,*p*]chrysenes derivatives.

We used GC-MS analysis to monitor the conversion of TPE to DPP in hexane and THF at concentrations of $10^{-3}$ and $10^{-4}$ M after 4 h of UV-light irradiation (302 nm, ≈5 mW cm$^{-2}$). Unfortunately, at $10^{-5}$ M the detection of the species under investigation was limited. The GC traces for the synthesised materials TPE and DPP were also obtained for reference purposes (Figure 7). From the corresponding ESI mass spectra (Figure 8), the peak at approximately 8.07 min in the GC-MS scan was found to represent TPE and that at approximately 10.25 min was found to represent DPP. GC-MS analysis of TPE in hexane ($10^{-4}$ M) after 4 h of UV-light irradiation and subsequent photo-oxidation shows that the TPE/DPP ratio is 67:33. The rate of photo-oxidation is faster in THF than in hexane, and consequently when TPE is dissolved in THF ($10^{-4}$ M) only DPP can be detected, which indicates near-complete photo-oxidation. For a concentration of $10^{-3}$ M, conversion to DPP is less than at a lower concentration, however, photo-oxidation conversion is still higher in THF (TPE: 56%, DPP: 44%) than in hexane (TPE: 78%, DPP: 22%). HPLC was also used to investigate the photo-oxidation of TPE-OCT in hexane after UV-light irradiation (4 h) and only one major peak was observed. It corresponded to 96% 3-(octyloxy)-9,10-diphenylphenanthrene (see below), which indicates almost complete photo-oxidation.

Owing to the observed solvent dependence we further investigated the changes in UV-visible absorbance and PL

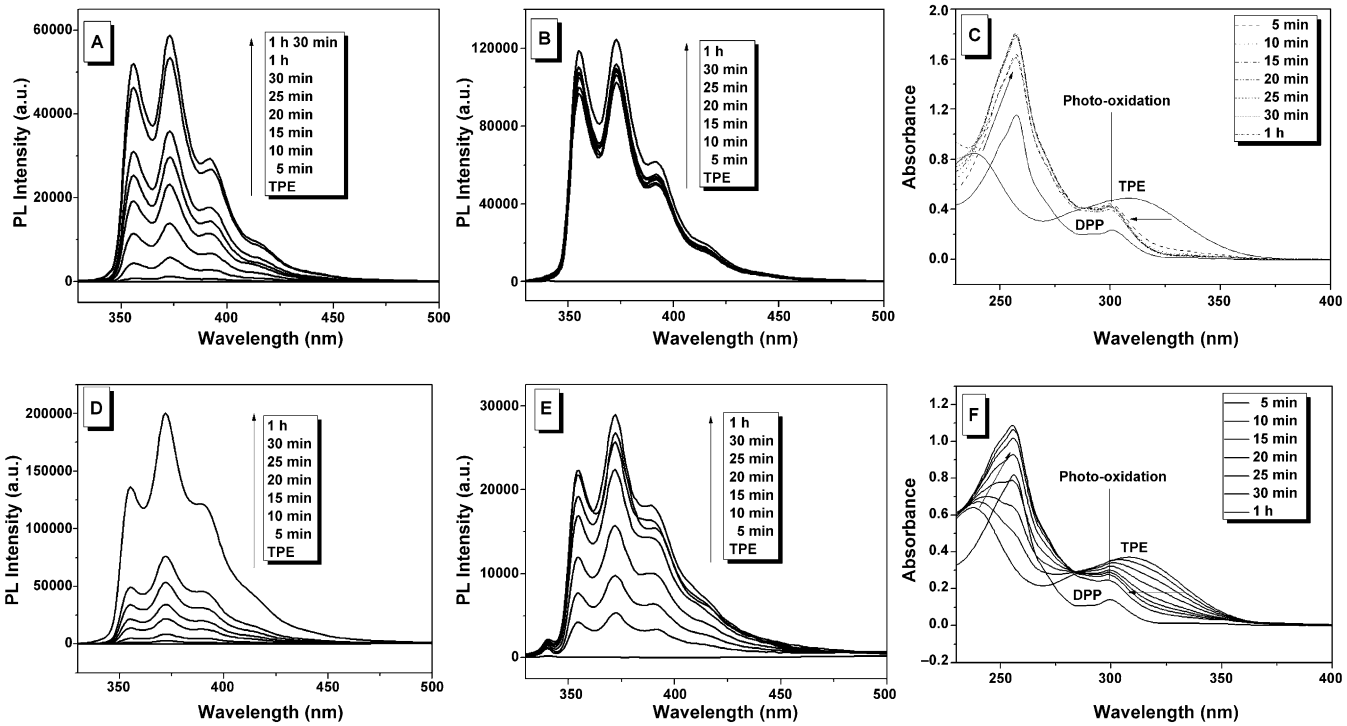


Figure 9. PL spectra of TPE in THF at A) $10^{-4}$ and B) $10^{-5}$ M, and C) the corresponding UV-visible spectra for $10^{-5}$ M; TPE in hexane at D) $10^{-4}$ and E) $10^{-5}$ M, and F) the corresponding UV-visible spectra for $10^{-5}$ M. UV-light exposure = 1 h, irradiation at 302 nm, approximately 5 mW cm$^{-2}$, $\lambda_{ex}$ = 310 nm.

emission of TPE in hexane and THF at both $10^{-4}$ and $10^{-5}$ M concentrations (5 mW cm$^{-2}$). The subsequent UV-visible and PL spectra during UV-light irradiation are shown in Figure 9. Unfortunately, we were unable to obtain the UV-visible time profiles at a concentration of $10^{-4}$ M owing to the high concentration. With regards to TPE in THF at $10^{-5}$ M (Figure 9B), the photo-oxidation seems to be near complete at only 5 min irradiation, with 5 min showing the sharpest increase in PL with only very slight changes after this time. At 5 min, the UV-visible spectra (Figure 9C) blueshifts and is identical to the pure synthesised DPP, which undoubtedly proves that DPP is the photo-oxidation product. After 1 h there is negligible change in the UV-visible and PL spectra. In contrast, at higher concentration ($10^{-4}$ M) the PL increases gradually up to 1.5 h, again with negligible changes in PL after this time. Therefore, similar to our GC-MS experiments photo-oxidation seems to be more efficient at lower concentration ($10^{-5}$ M) than at high concentration ($10^{-4}$ M).

The rates of oxidation in hexane (Figure 9D–F) are comparatively slower than those in THF at both concentrations. The UV-visible spectra at $10^{-5}$ M (Figure 9F) show only a slow gradual change during UV irradiation, which seems to be near complete after 30 min because after this time there is very little enhancement in the PL intensity. Again, there is negligible change in PL after 1 h. The corresponding UV-visible spectra show a gradual blueshift with UV-light irradiation and the UV-visible spectrum at 30 min is nearly identical to that of DPP. At higher concentration ($10^{-4}$ M), even after 1 h the photo-oxidation is not complete and the PL intensity keeps rising (not shown in Figure 9D). Therefore, from the PL spectra we can safely say that the photo-oxidation is concentration and solvent dependent: a low concentration and using THF as the solvent favours a fast rate of photo-oxidation. The APCI mass spectra before and after UV-light irradiation of TPE-OCT and TPE-PEG in hexane and THF, respectively, are shown in Figure S1 of the Supporting Information. This confirms that the photo-oxidation products are phenanthrene-based. The mass spectra of TPE-PEG shows a Gaussian distribution of molecular ions because of the polydispersity of TPE-PEG owing to the different number of ethylene glycol units $(CH_2CH_2O)_n$ in the side chain, with an average number of $n = 12$. From cyclic-voltammetry measurements the oxidation potentials of TPE-OCT and TPE were calculated as 0.78 and 0.89 V, respectively. The lower oxidation potential of TPE-OCT than that of TPE is due to the positive inductive effect ($+I$) of the ether group. A similar observation was made by Rathore's group regarding the oxidation of tetraphenylethene derivatives using DDQ/$MeSO_3H$, in which they reported longer reaction times for the derivatives with higher oxidation potentials.[19] Most water-soluble TPE-based materials used in biosensor applications are functionalised with $+I$ functional groups.

The electron-donating oxygen atom in TPE-OCT lowers the oxidation potential of TPE-OCT relative to that of TPE, which therefore results in faster rates of photo-oxidation of TPE-OCT than of TPE in both hexane and THF (Figure 5). In a 99% water/THF solvent mixture (Figure 6) we observed more "over-oxidation" in TPE-OCT and TPE-PEG

compared with only a slight "over-oxidation" in TPE, although the rates of photo-oxidation look similar. With regards to TPE and TPE-OCT, the fluorescence decreases as shown in the photos (Figure 6) and the decrease of the emission peak around 450-500 nm shown in the PL spectra. TPE-PEG was synthesised to compare its photo-oxidation with TPE-OCT in an aqueous environment. In a 99% water/THF solvent mixture, TPE-PEG is dissolved (although aggregation still takes place) and TPE-OCT is a "nano-suspension". From the PL spectra, we can see that during UV-light irradiation the broad emission around 475 nm decreases and a more defined (0,0 0,1 and 0,2) blueshifted emission around 375 nm increases, which is related to diphenylphenanthrene. These blueshifted phenanthrene peaks are strong in TPE-PEG and very weak in TPE-OCT. Why? The conversion of TPE-OCT to its diphenylphenanthrene analogue induces ACQ, therefore, in the nanoparticle the fluorescence is weak. However, although TPE-PEG is "aggregated" in the water, it is also solvated and, therefore, the conversion of TPE-PEG to its phenanthrene analogue does not induce ACQ.

**PMMA matrix**: The concentration dependence was further investigated by dispersing TPE at different weight percentages (1, 5 and 9 wt%) in a PMMA solid matrix and monitoring the change in PL intensity at 372 nm. The resulting kinetic scans are shown in Figure 10 and clearly illustrate

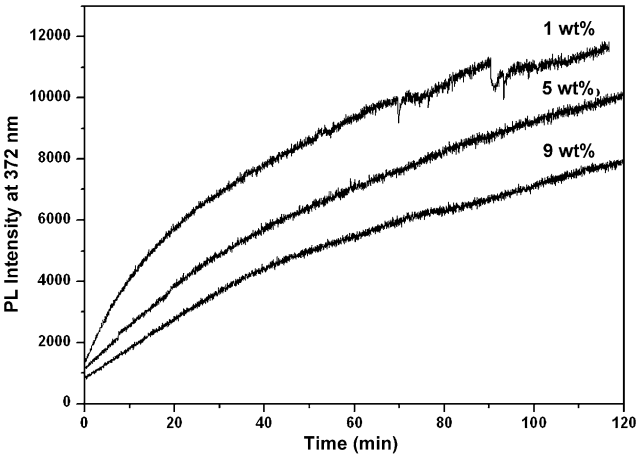


Figure 10. The kinetic scans of TPE-PMMA thin films on quartz substrates at different TPE concentration, during 2 h UV-light irradiation at excitation at 310 nm.

that as the weight percentage of TPE is increased the rate of oxidation decreases. The corresponding PL spectra and UV-visible spectra (Figure 11) clearly show the transformation of TPE into DPP at all three weight percentage concentrations.

Owing to the probable excimer formation at high concentrations of DPP we did not exceed 9 wt% TPE, which could compromise the validity of our results and interpretation.

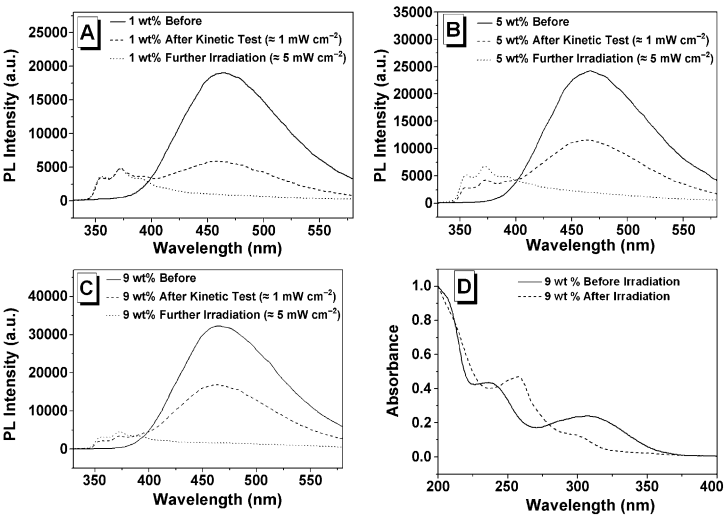


Figure 11. PL spectra of TPE-PMMA at different wt% TPE: A) 1, B) 5 and C) 9 wt% during different stages of UV-light irradiation. D) UV-visible spectra of 9 wt% before and after approximately 5 mW cm$^{-2}$ irradiation. Further irradiation was conducted for 30 min at 302 nm. All thin films were prepared on quartz substrates, spin-coated from dichloromethane.

From the PL spectrum shown in Figure 4, excimer formation at 9 wt% DPP in PMMA is negligible.

The photochemistry of tetraphenylethene and stilbene are very similar and tetraphenylethene photo-oxidation proceeds in a similar manner to that of stilbene-based materials. In our case no oxidant was used, only solvents and UV light, so the oxygen from the air and subsequently in the solvent is enough to allow the oxidation to proceed. The small concentration of the fluorophore means that only a trace of oxidant is necessary and the oxygen in the solvent is enough to trap the trans-4*a*,4*b*-dihydrodiphenylphenanthrene and oxidise it to 9,10-diphenylphenanthrene (Figure 12).

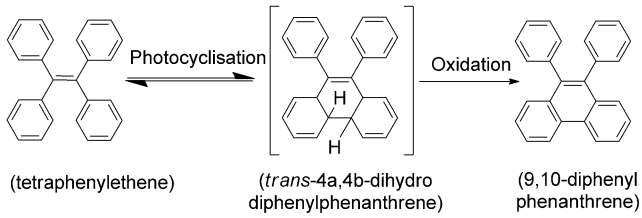


Figure 12. Photocyclisation and oxidation of tetraphenylethene.

## Conclusion

We have investigated the optical properties and photo-oxidation behaviour of TPE and its derivatives in solution and the "aggregate" state. AIE has been observed for all the TPE derivatives and the opposite behaviour, namely, ACQ, has been observed for the oxidised derivative of TPE, that is, 9,10-diphenylphenanthrene. From mass spectrometry, UV-visible absorption and photoluminescence we have dem-

onstrated that upon UV-light exposure the TPE compounds oxidise to their diphenylphenanthrene derivatives. We hope that this study will encourage the design and synthesis of more photostable TPE derivatives, possibly with electron-withdrawing groups, thus decreasing their susceptibility to photo-oxidation.

## Acknowledgements

This work was financially supported by the NSFC (20874025, 21174045). M.P.A is the awardee of a NSFC Research Fellowship for International Young Scientists (21150110141) and the Key Fellowship of China Postdoctoral Science Foundation (20100480065). The Open Program for Beijing National Laboratory for Molecular Sciences (BNLMS) and the Fundamental Research Funds for the Central Universities (HUST2010MS101) are also thanked. Finally we thank the Analysis and Test Center of Huazhong University of Science and Technology for support.

[1] a) J. D. Luo, Z. L. Xie, J. W. Y. Lam, L. Cheng, H. Y. Chen, C. F. Qiu, H. S. Kwok, X. W. Zhan, Y. Q. Liu, D. Zhu, B. Z. Tang, *Chem. Commun.* **2001**, 1740–1741.

[2] a) J. W. Chen, B. Xu, X. Y. Ouyang, B. Z. Tang, Y. Cao, *J. Phys. Chem. A* **2004**, *108*, 7522–7526; b) K. Itami, Y. Ohashi, J.-I. Yoshida, *J. Org. Chem.* **2005**, *70*, 2778–2792; c) K. Itami, J.-I. Yoshida, *Chem. Eur. J.* **2006**, *12*, 3966–3974; d) Q. Zeng, Z. Li, Y. Q. Dong, C. A. Di, A. J. Qin, Y. N. Hong, L. Ji, Z. C. Zhu, C. K. W. Jim, G. Yu, Q. Q. Li, Z. A. Li, Y. Q. Liu, J. G. Qin, B. Z. Tang, *Chem. Commun.* **2007**, 70–72.

[3] a) Y. N. Hong, J. W. Y. Lam, B. Z. Tang, *Chem. Commun.* **2009**, 4332; b) Y. N. Hong, J. W. Y. Lam, B. Z. Tang, *Chem. Soc. Rev.* **2011**, *40*, 5361–5388.

[4] a) M. P. Aldred, C. Li, G. F. Zhang, W. L. Gong, A. D. Q. Li, Y. Dai, D. Ma, M. Q. Zhu, *J. Mater. Chem.* **2012**, *22*, 7515–7528; G. F. Zhang, M. P. Aldred, W. L. Gong, C. Li, M. Q. Zhu, *Chem. Commun.* **2012**, *48*, 7711–7713.

[5] a) W. Z. Yuan, P. Lu, S. M. Chen, J. W. Y. Lam, Z. M. Wang, Y. Liu, H. S. Kwok, Y. G. Ma, B. Z. Tang, *Adv. Mater.* **2010**, *22*, 2159–2163; b) Y. Liu, S. M. Chen, J. W. Y. Lam, F. Mahtab, H. S. Kwok, B. Z. Tang, *J. Mater. Chem.* **2012**, *22*, 5184–5189; c) C. Y. K. Chan, Z. J. Zhao, J. W. Y. Lam, J. Z. Liu, S. M. Chen, P. Lu, F. Mahtab, X. J. Chen, H. H. Y. Sung, H. S. Kwok, Y. G. Ma, I. D. Williams, K. S. Wong, B. Z. Tang, *Adv. Funct. Mater.* **2012**, *22*, 378–389; d) J. Huang, N. Sun, J. Yang, R. L. Tang, Q. Q. Li, D. G. Ma, J. G. Qin, Z. Li, *J. Mater. Chem.* **2012**, *22*, 12001–12007; e) J. Huang, X. Yang, J. Y. Wang, C. Zhong, L. Wang, J. G. Qin, Z. Li, *J. Mater. Chem.* **2012**, *22*, 2478–2484.

[6] J. H. Burroughes, D. D. C. Bradley, A. R. Brown, R. N. Marks, K. Mackay, R. H. Friend, P. L. Burns, A. B. Holmes, *Nature* **1990**, *347*, 539–541.

[7] a) Y. Liu, C. M. Deng, L. Tang, A. J. Qin, R. R. Hu, J. Z. Sun, B. Z. Tang, *J. Am. Chem. Soc.* **2011**, *133*, 660–663; b) Y. Liu, A. J. Qin, X. J. Chen, X. Y. Shen, L. Tong, R. R. Hu, J. Z. Sun, B. Z. Tang, *Chem. Eur. J.* **2011**, *17*, 14736–14740; c) M. Wang, G. X. Zhang, D. Q. Zhang, D. B. Zhu, B. Z. Tang, *J. Mater. Chem.* **2010**, *20*, 1858–1867; d) Y. N. Hong, H. Xiong, J. W. Y. Lam, M. Haussler, J. Z. Liu, Y. Yu, Y. C. Zhong, H. H. Y. Sung, I. D. Williams, K. S. Wong, B. Z. Tang, *Chem. Eur. J.* **2010**, *16*, 1232–1245; e) X. G. Gu, G. X. Zhang, D. Q. Zhang, *Analyst* **2012**, *137*, 365–369; f) M. Nakamura, T. Sanji, M. Tanaka, *Chem. Eur. J.* **2011**, *17*, 5344–5349; g) T. Sanji, K. Shiraishi, M. Nakamura, M. Tanaka, *Chem. Asian J.* **2010**, *5*, 817–824.

[8] a) L. Liu, G. X. Zhang, J. F. Xiang, D. Q. Zhang, D. B. Zhu, *Org. Lett.* **2008**, *10*, 4581–4584; b) X. R. Wang, J. M. Hu, T. Liu, G. Y. Zhang, S. Y. Liu, *J. Mater. Chem.* **2012**, *22*, 8622–8628; c) F. Sun, G. X. Zhang, D. Q. Zhang, L. Xue, H. Jiang, *Org. Lett.* **2011**, *13*, 6378–6381; d) Y. N. Hong, S. J. Chen, C. W. T. Leung, J. W. Y. Lam, J. Z. Liu, N. W. Tseng, R. T. K. Kwok, Y. Yu, Z. K. Wang, B. Z. Tang, *ACS Appl. Mater. Interfaces* **2011**, *3*, 3411–3418.

[9] a) S. Sharafy, K. A. Muszkat, *J. Am. Chem. Soc.* **1971**, *93*, 4119–4125; b) G. Fischer, G. Seger, K. A. Muszkat, E. Fischer, *J. Chem. Soc. Perkin Trans. 2* **1975**, 1569–1576; c) P. F. Barbara, S. D. Rand, P. M. Rentzepis, *J. Am. Chem. Soc.* **1981**, *103*, 2156–2162; d) H. Goerner, *J. Phys. Chem.* **1982**, *86*, 2028–2035; e) C. L. Schilling, E. F. Hilinski, *J. Am. Chem. Soc.* **1988**, *110*, 2296–2298; f) D. A. Shultz, M. A. Fox, *J. Am. Chem. Soc.* **1989**, *111*, 6311–6320; g) J. Morais, J. Ma, M. B. Zimmt, *J. Phys. Chem.* **1991**, *95*, 3885–3888; h) Y. P. Sun, M. A. Fox, *J. Am. Chem. Soc.* **1993**, *115*, 747–750.

[10] a) G. X. Huang, B. D. Ma, J. M. Chen, Q. Peng, G. X. Zhang, Q. H. Fan, D. Q. Zhang, *Chem. Eur. J.* **2012**, *18*, 3886–3892; b) C. E. Bunker, N. B. Hamilton, Y. P. Sun, *Anal. Chem.* **1993**, *65*, 3460–3465.

[11] a) N. Tamai, H. Miyasaka, *Chem. Rev.* **2000**, *100*, 1875–1890; b) J. Quenneville, T. J. Martinez, *J. Phys. Chem. A* **2003**, *107*, 829–837; c) A. Momotake, T. Arai, *J. Photochem. Photobiol. C* **2004**, *5*, 1–25; d) R. J. Sension, S. T. Repinec, A. Z. Szarka, R. M. Hochstrasser, *J. Chem. Phys.* **1993**, *98*, 6291–6315.

[12] K. B. Jørgensen, *Molecules* **2010**, *15*, 4334–4358.

[13] A. J. Qin, L. Tang, J. W. Y. Lam, C. K. W. Jim, Y. Yu, H. Zhao, J. Z. Sun, B. Z. Tang, *Adv. Funct. Mater.* **2009**, *19*, 1891–1900.

[14] H. Tong, Y. N. Hong, Y. Q. Dong, M. Haussler, J. W. Y. Lam, Z. Li, Z. F. Guo, Z. H. Guo, B. Z. Tang, *Chem. Commun.* **2006**, 3705–3707.

[15] a) X. Q. Zhang, Z. G. Chi, H. Y. Li, B. J. Xu, X. F. Li, S. W. Liu, Y. Zhang, J. R. Xu, *J. Mater. Chem.* **2011**, *21*, 1788–1796; b) H. Y. Li, Z. G. Chi, B. J. Xu, X. Q. Zhang, X. F. Li, S. W. Liu, Y. Zhang, J. R. Xu, *J. Mater. Chem.* **2011**, *21*, 3760–3767.

[16] Y. Nakamura, T. Tsuihiji, T. Mita, T. Minowa, S. Tobita, H. Shizuka, J. Nishimura, *J. Am. Chem. Soc.* **1996**, *118*, 1006–1012.

[17] F. B. Mallory, C. S. Wood, J. T. Gordon, *J. Am. Chem. Soc.* **1964**, *86*, 3094–3102.

[18] L. Liu, B. Yang, T. J. Katz, M. K. Poindexter, *J. Org. Chem.* **1991**, *56*, 3769–3775.

[19] T. S. Navale, K. Thakur, R. Rathore, *Org. Lett.* **2011**, *13*, 1634–1637.

Received: July 29, 2012
Revised: September 4, 2012
Published online: ■■ ▮▮, 0000

  

Fluorophores

*M. P. Aldred, C. Li,*
*M.-Q. Zhu**..... ▮▮▮▮–▮▮▮▮

**Optical Properties and Photo-Oxidation of Tetraphenylethene-Based Fluorophores**

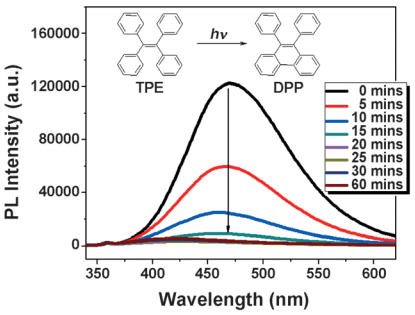


**Photo finish**: The optical properties and photo-oxidation of tetraphenylethene (TPE) and its derivatives in solution, the nanoparticle state and in a PMMA matrix are discussed (see scheme). This demonstration should be useful in encouraging the design of more photostable TPE molecules that are commonly used in biosensing and imaging research.